Luo, Y., and Korenaga, J., 2021, Efficiency of eclogite removal from continental lithosphere and its implications for cratonic diamonds: Geology, v. 49, https://doi.org/10.1130/G48204.1.

Supporting information for:

Efficiency of eclogite removal from continental lithosphere and its implications for cratonic diamonds

Yantao Luo[1] and Jun Korenaga[1]

[1]The Department of Earth and Planetary Sciences, Yale University, PO Box 208109, New Haven, Connecticut 06520-8109, USA. Email addresses: yantao.luo@yale.edu and jun.korenaga@yale.edu

Contents of this file:

Model parameters

Figure S1 to S3

1. MODEL PARAMETERS

Temperature dependent thermal conductivities

Crust (Whittington et al., 2009):

$$k(T < 846K) = 2700 * \frac{199.5 + 0.0857 * T - 5 * 10^{6} * T^{-2}}{0.21178} * \frac{(567.3 * T^{-1} - 0.062)}{10^{6}}$$

$$k(T > 846K) = 2700 * \frac{229.32 + 0.0323 * T - 47.9 * 10^{-6} * T^{2}}{0.22178} * \frac{(0.732 - 1.35 * 10^{-4} * T)}{10^{6}}$$

Mantle (McKenzie et al., 2005):

$$k(T) = \frac{5.3}{1 + 0.0015 * (T - 273)} + 1.753 * 10^{-2} - 1.0365 * 10^{-4} * T + 2.2451 * 10^{-7} * T^{2} - 3.4071 * 10^{-11} * T^{3}$$

Radiogenic heat production in cratons (calculated based on Rudnick et al., 1998)

	^{235}U (ppm)	^{238}U (ppm)	^{232}Th (ppm)	^{40}K (ppm)	Present Heat Production (μW m-3)
Bulk continental crust	$4.9*10^{-3}$	0.70	3.0	1.2	0.51
Lithospheric mantle	$2.6*10^{-4}$	0.037	0.14	0.043	0.028

The continental crust is divided into upper, middle, and lower one thirds, with 60%, 34%, and 6% of total crust heat production, respectively.

Dislocation creep constants (Jain et al., 2019)

Model OL-DB_2 for dry diffusion and dry dislocation is used.

For diffusion, $p = 2.11 \pm 0.15, E = 370 \pm 15$ kJ/mol, $A = 10^{7.86\pm0.15}$.

For dislocation, $n = 3.64 \pm 0.99, E = 424 \pm 23$ kJ/mol, $A = 10^{2.10\pm0.20}$.

The mean value is used for each parameter. Preexponential factors A listed above are calibrated at 1523 K and 0.3 GPa with activation volume $V = 0$. We recalibrated the preexponential factor for every activation volume tested in this study as follows:

	$A_{diffusion}$	$A_{dislocation}$
$V = 10\ cm^3$	$10^{7.78}$	$10^{2.20}$
$V = 20\ cm^3$	$10^{7.89}$	$10^{2.31}$
$V = 30cm^3$	$10^{7.99}$	$10^{2.41}$

2. SUPPORTING FIGURES

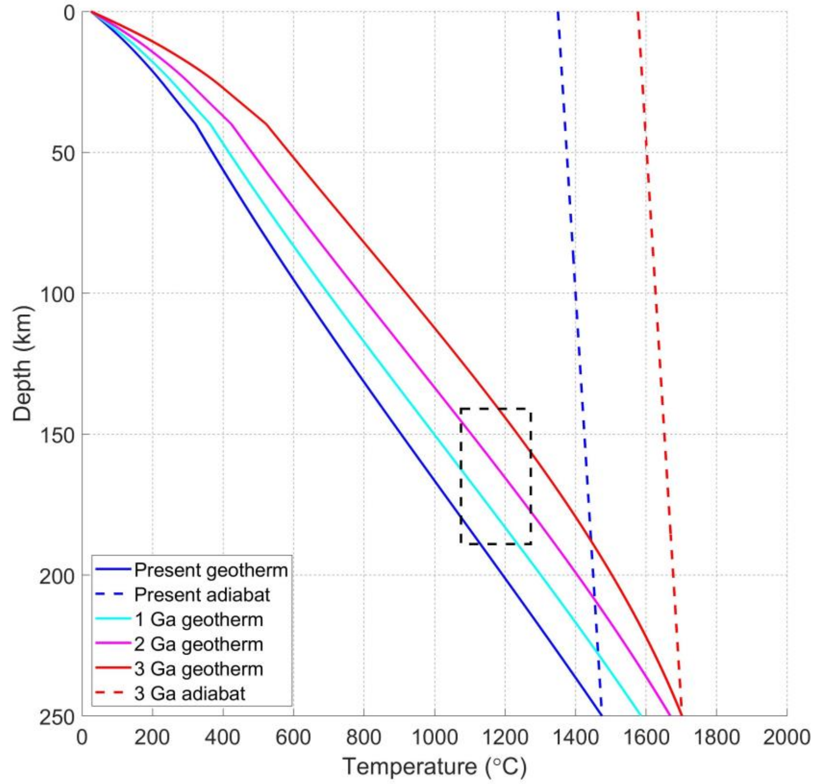

Figure S1. Calculated current, 1 Ga, 2 Ga, and 3 Ga geotherms are plotted with current and 3 Ga adiabat lines. Dashed rectangle represents the constraints from the geothermometry of cratonic diamonds, 1174 ± 99 ℃ at 55 ± 8 kbar (Stachel and Harris, 2008).

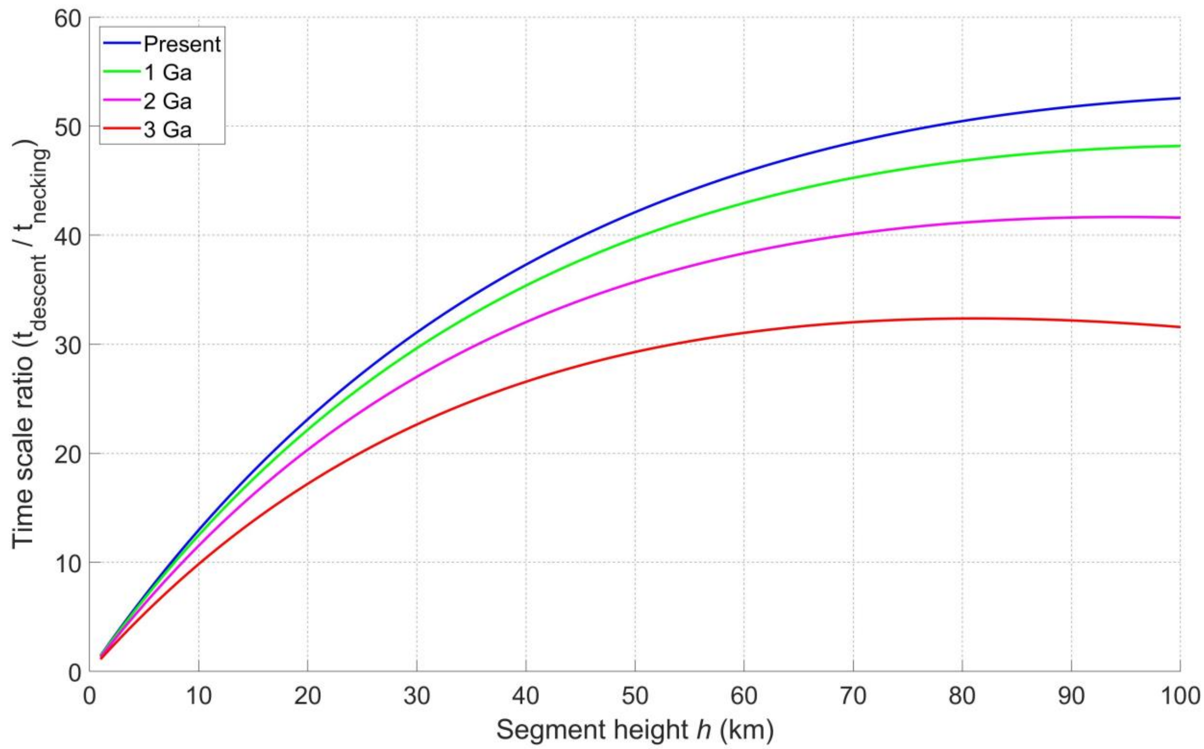

Figure S2. The ratio of the time scale for a segment to descend over the time scale for the growth of necking instability is plotted as a function of segment height h. The descent time scale is based on eq. (8) in the main text. The time scale for necking instability is estimated as $t = \left((n-1) * \dot{\epsilon}\right)^{-1}$ based on eq. (6) in Zuber and Parmentier (1986). $\dot{\epsilon}$ is the strain rate generated by differential velocity, and n is the stress exponent of the material, where we use $n = 3.5$ for eclogite (Zhang and Green, 2007). Necking instability grows exponentially from infinitesimal perturbations, and segmentation would take place when the ratio >> 1.

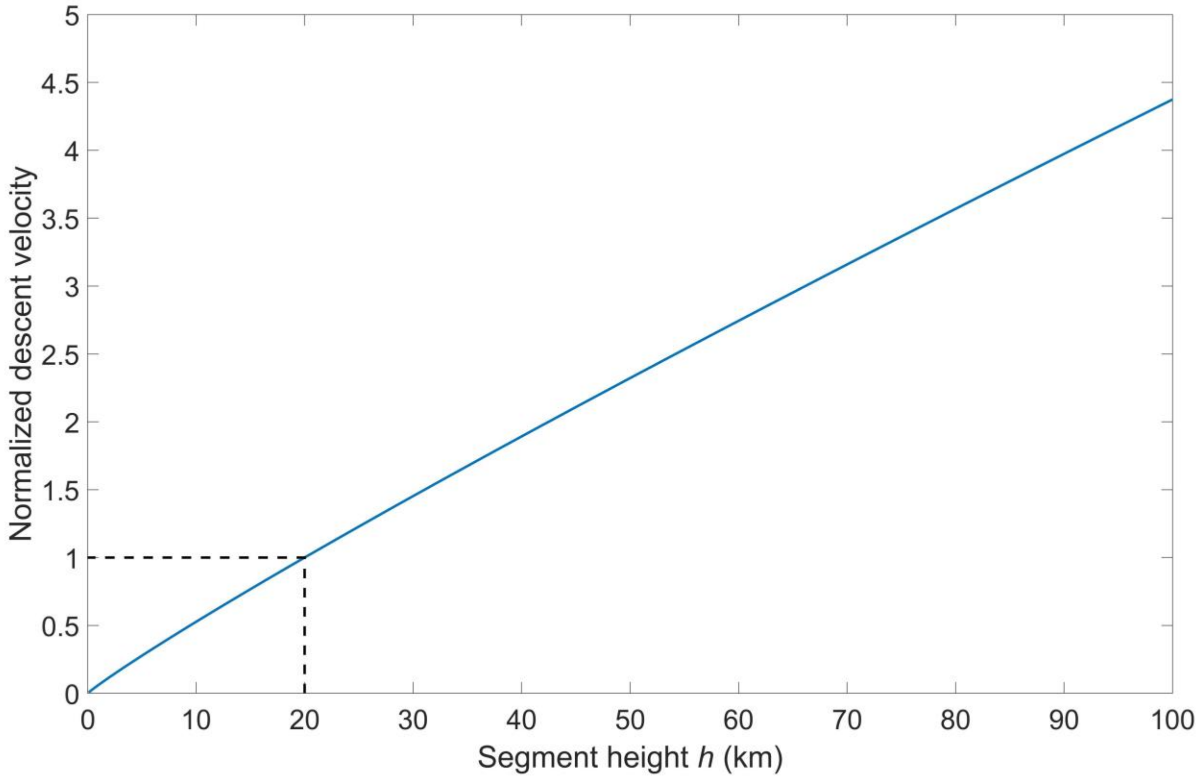

Figure S3. Descent velocities calculated with a range of segment heights are normalized regarding to the result of 20 km height, with other parameters fixed at $L = 2500$ km, $w = 7$ km, $\eta = 2 * 10^{30}$ N·m, and $\Delta\rho = 200$ g/cm^3.

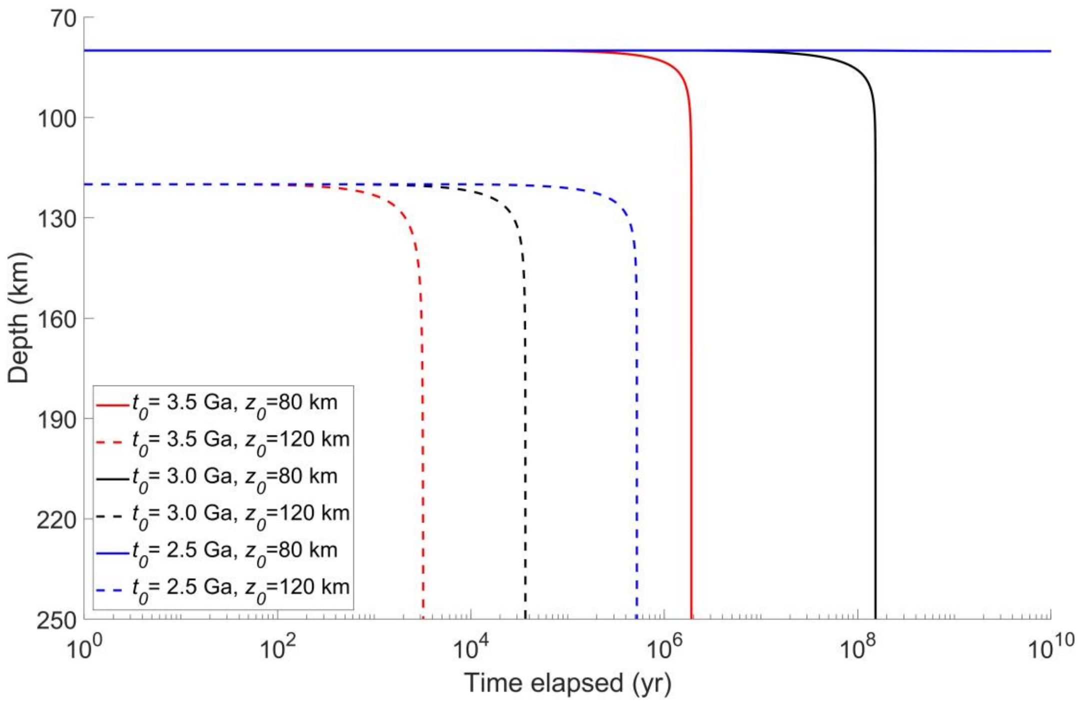

Figure S4. The depth of oceanic crust fragments with different incorporation ages and starting depths is plotted as a function of the time elapsed after incorporated into CLM. An activation volume V of 20 cm^3/mol for the dislocation creep regime and a segment height h of 20 km are used for this plot. Each of the curves in this plot corresponds to a point in Figure 3, and the time elapsed until the curst fragments descend to 250 km is the escape time shown in Figure 3.

REFERENCES CITED

Jain, C., Korenaga, J., and Karato, S. i., 2019, Global analysis of experimental data on the rheology of olivine aggregates: Journal of Geophysical Research: Solid Earth, v. 124, no. 1, p. 310-334.

McKenzie, D., Jackson, J., and Priestley, K., 2005, Thermal structure of oceanic and continental lithosphere: Earth and Planetary Science Letters, v. 233, no. 3, p. 337-349, https://doi.org/10.1016/j.epsl.2005.02.005.

Rudnick, R. L., McDonough, W. F., and O'Connell, R. J., 1998, Thermal structure, thickness and composition of continental lithosphere: Chemical Geology, v. 145, no. 3, p. 395-411, https://doi.org/10.1016/S0009-2541(97)00151-4.

Stachel, T., and Harris, J. W., 2008, The origin of cratonic diamonds — Constraints from mineral inclusions: Ore Geology Reviews, v. 34, no. 1, p. 5-32, https://doi.org/10.1016/j.oregeorev.2007.05.002.

Whittington, A. G., Hofmeister, A. M., and Nabelek, P. I., 2009, Temperature-dependent thermal diffusivity of the Earth’s crust and implications for magmatism: Nature, v. 458, no. 7236, p. 319-321, 10.1038/nature07818.

Zhang, J., and Green, H. W., 2007, Experimental Investigation of Eclogite Rheology and Its Fabrics at High Temperature and Pressure: Journal of Metamorphic Geology, v. 25, no. 2, p. 97-115, 10.1111/j.1525-1314.2006.00684.x.

Zuber, M. T., and Parmentier, E. M., 1986, Lithospheric necking: a dynamic model for rift morphology: Earth and Planetary Science Letters, v. 77, no. 3, p. 373-383, https://doi.org/10.1016/0012-821X(86)90147-0.